Available online at www.sciencedirect.com

ScienceDirect

Energy Procedia 4 (2011) 5299–5305

Energy Procedia

www.elsevier.com/locate/procedia

GHGT-10

Assessment of fracture connectivity and potential for CO_2 migration through the reservoir and lower caprock at the In Salah storage site

James Smith, Sevket Durucan*, Anna Korre, Ji-Quan Shi, Caglar Sinayuc

Department of Earth Science and Engineering, Royal School of Mines, Imperial College London, Prince Consort Road, London SW7 2BP, UK

Abstract

Fractures are thought to strongly affect the flow of CO_2 at the In Salah storage site. In the work presented here, fracture networks at In Salah are characterised and modelled to assess percolation. Available fracture data is considered in the context of general characteristics of other fracture networks and this data is then used to model potential realisations of fracture networks within the In Salah reservoir and lower caprock. Horizontal percolation of fracture networks is highly dependent on fracture length, the proportion of cemented fractures and the properties of the uncharacterised disperse fracture set. However, largely open fractures with length distributions exceeding calculated values will percolate within the reservoir and lower caprock. Injection induced stress changes are assessed with a coupled flow geomechanical model. Both tensile and shear failure of fractures are found to be unlikely but possible given certain combinations of conditions.

Keywords: CO_2 Storage; In Salah; Fracture; Stress

1. Introduction

The In Salah site in Algeria produces gas reserves within a thin Carboniferous sandstone and siltstone reservoir. This is overlain first by Carboniferous silty mudstones forming the lower and upper caprock and then by Cretaceous sandstones and mudstone of the Pan Saharan aquifer. The reservoir and lower caprock taken together are referred to as the storage complex. The produced natural gas contains between 1 and 9 % CO_2 and so on separation, the CO_2 is injected back into the aquifer-leg of the reservoir at three separate locations (KB-501, KB-502 and KB-503) since August 2004. A site map and the location of injection and production wells are shown in Figure 1. As the injection site is also a producing gas field, the storage formation is relatively well characterised. It is known that fractures exist in the region and these have been observed at KB-502 and an injection well, Kb-14 [1]. The fracture data from these wells is shown in Figure 2a and a schematic diagram of fracturing in the region is shown in Figure 2b. This data indicates similar fracturing to be present in the reservoir and lower caprock section with uncharacterised fracturing in the upper caprock. An enhanced pathway of migrating CO_2 from the Kb-502 injector towards the NW leading to breakthrough of CO_2 at the suspended (now fully decommissioned) appraisal well KB-5 [2] indicates that CO_2 transport in the reservoir cannot be explained by matrix flow alone. Pressure history matching leads to the same conclusion and, as a result, it is expected that fractures and/or faults contribute significantly to the permeability of the region.

Within the reservoir, both the matrix and fractures can contribute to permeability, even if the fractures are unconnected. However, within the lower caprock, where matrix permeability is very low, any flow is likely to be a result of fracture permeability alone. A precondition for a fracture network to be permeable in an impermeable matrix is for a connecting pathway of open fractures to exist. This property of a fracture network is known as percolation. For flow to occur in a percolating fracture network requires any capillary entry pressures for the pathway to be overcome. The production of trapped hydrocarbons at In Salah is indicative of a sealing caprock, therefore, it is believed that fractures do not form a significant leakage pathway out of the storage complex. This indicates either the absence of a vertically percolating pathway through a significant portion of the caprock or capillary sealing of such a pathway. However, it is not known whether fracture networks within the storage complex are percolating and what changes these fracture networks may undergo during injection of CO_2.

* Corresponding author. Tel.: +44-20-7594-7354; fax: +44-20-7594-7354.
E-mail address: s.durucan@imperial.ac.uk

doi:10.1016/j.egypro.2011.02.510

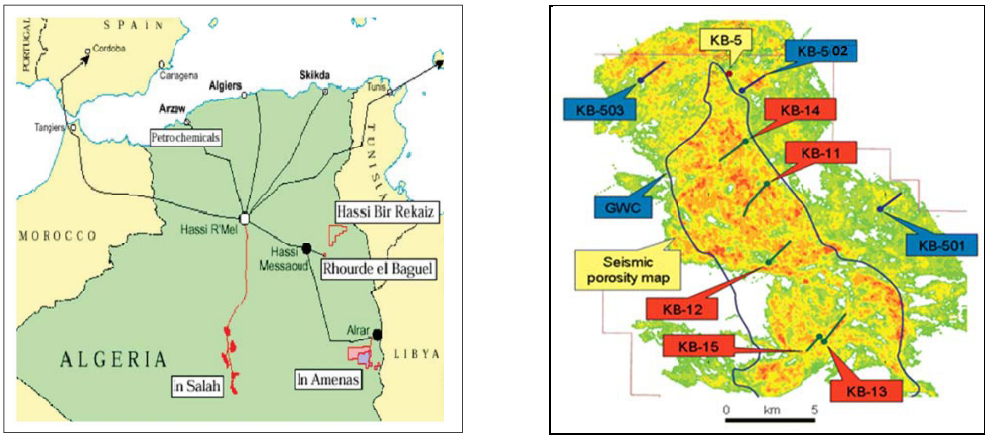

Figure 1. Map showing (a) the location of In Salah field; (b) Krechba site and the three CO_2 injection wells (KB501, KB502 and KB503) and the five production wells (KB-11, KB-12, KB-13, KB-14 and KB-15) [3].

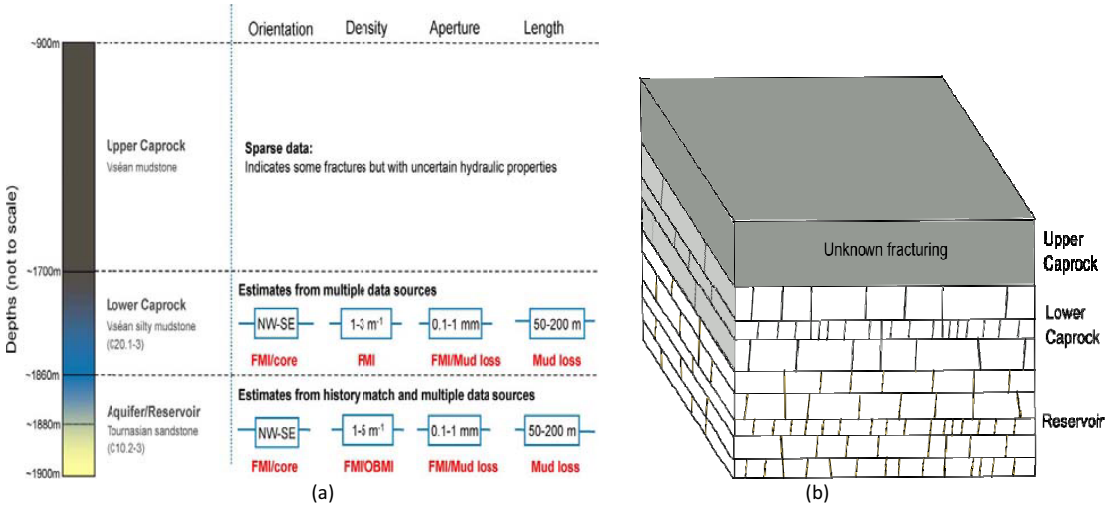

Figure 2. (a) Fracture orientation, density, aperture and length data acquired from KB-502 and KB-14 [1]; (b) Schematic diagram of fractures in the reservoir and caprock (Not to scale).

Modelling of the fracture network around KB-502 and KB-14 has been carried out by Iding & Ringrose [1]. Their fracture data is shown in Figure 2a. In this paper, their fracture data is considered in the context of general characteristics of fracture networks derived from other field measurements. Using this data, large numbers of realisations of the possible fracture networks are modelled to investigate the uncertainties in the occurrence of fracture network percolation within the storage complex. Furthermore, injection induced changes to these fracture networks are investigated using coupled flow-geomechanical models.

2. In Salah fracture data and general fracture characteristics

Fractures can be defined by orientation, aperture, spatial distribution, shape and size. Fracture orientation data [1], suggests a dominant fracture orientation of NW-SE about which there is approximately 30° of uniform variation. The reliability of this data is high as it is acquired from multiple sources. Fracture density data, Figure 2a, can be considered reliable around the well that it was acquired from. However, density may vary significantly over a wider region. For instance, seismic surveys suggest the possible existence of a fault in the region of KB-502/KB-5 [2] around which fracture density is likely to be greater.

Fracture length data at In-Salah, shown in Figure 2a, is acquired from mud loss events. Mud loss length estimation only provides information on the most conductive and therefore longest fractures. Also the length estimate from mud losses could be a sum of multiple fractures. Field data from other sources [4] suggests that fracture length typically (L) follows a power-law distribution $f(L) = \alpha L^{-m}$. A power-law distribution is defined by values of the maximum length (L_{max}), minimum length (L_{min})

and the power-law exponent (m) while α is found through normalisation. These parameters have not been characterised at In-Salah.

The data on fracture apertures, shown in Figure 2a, is acquired using FMI and mud loss data although there are potentially large uncertainties in these measurements [1]. Additionally, core analysis data shows that some fractures are cemented and therefore not conductive although the number of closed fractures is not reported [1]. Field measurements at other sites show that aperture follows a power-law distribution [5, 6] and that aperture is correlated with length [7, 8]. Therefore the most conductive fractures are also the most extensive and dominate the flow characteristics of the media.

During formation, the propagation of fractures can be truncated by stratigraphic layer boundaries. Image log data from KB-14 shows stratigraphic zonation of fractures [1], which suggests that they are stratabound to some extent. The layer thickness will therefore confine the vertical extent of some fractures although other fractures in a largely stratabound set may propagate through layer boundaries. The layer truncation percentage (P_{trunc}) of a stratabound set is defined as the percentage of fractures that propagate through a layer boundary. Larger fractures are the most likely to propagate through a layer boundary. If P_{trunc} is equal to zero then vertical permeability will be zero while a non-zero value of P_{trunc} provides the possibility of vertical permeability.

3. Injection induced changes in fracture properties

Injection of CO_2 into the reservoir causes the pressure and stress to increase. As the pressure change is greater than the stress change, the effective stress will decrease. This injection induced stress change depends on the volume of CO_2 injected, permeability, compressibility, effective storage volume, elastic moduli and the degree of confinement. Lower values of permeability (k) lead to greater pressure changes. Higher values of Young's modulus (E) and Poisson ratio (υ) lead to greater stress changes with the value of υ particularly affecting the horizontal stress changes. The decrease in effective stress leads to an increase in matrix porosity and fracture aperture which in turn causes an increase in permeability. The relationship between fracture aperture and normal effective stress depends on the fracture stiffness. Laboratory and field data from other sources [9, 10] typically found that the stiffness and normal stress are positively correlated. If the effective stress decrease is great enough then the rock matrix or fractures may undergo geomechanical failure [11]. There are two relevant types of geomechanical failure. Tensile failure of a fracture conservatively occurs when the pressure of fluid within a fracture (P) exceeds the normal stress on the fracture (σ). Shear failure of a fracture occurs when shear stress on a fracture (τ) reaches the value shown in Equation 1, where θ is the angle of internal friction and σ' is the effective normal stress.

$$\tau = \sigma' \times tan\theta \tag{1}$$

4. Fracture network modelling and percolation assessment

The objective of this study was to investigate the occurrence of percolation in fracture networks in the reservoir and lower caprock at In Salah. This is performed by modelling large numbers of potential realisations of the fracture networks using the data and fracture characteristics described in Section 2. As previously discussed, there are numerous uncertainties in the knowledge of fracture properties that are used to define fracture network models. Density and orientation are reasonably well characterised. However, length and aperture are not well characterised and so it is the effect of these properties on percolation that is investigated.

Fracture modelling is performed using a marked point process methodology. Marked point processes have been widely used in fracture modelling [12, 13, 14, 15] and the methodology is described in detail in the context of CO_2 storage by Smith et al. [16]. In the modelling, each fracture is defined by a spatial location and a number of marks describing orientation, aperture and size. Fractures are stochastically assigned to a model region based on the distributions of measured properties and some assumptions about general fracture properties. Realistic fracture characteristics such as clustering, truncation and forbidden zones can be incorporated into the modelling.

A horizontal model domain of 1km × 1km is defined with 5 vertical layers. The model domain is considered to represent a section of the reservoir and lower caprock as they have very similar fracture properties. Stratabound fractures are assumed and thin layers of constant vertical thickness are defined. The layer thickness will not affect the results without currently unavailable data on density variation between layers. Fractures are assumed to be Poisson distributed and the line density for each realisation is selected from the range 1 - 5 m^{-1}. A uniform strike distribution of NW-SE ± 15° and a dip value of 86° are used for each realisation. As fractures are largely stratabound, fracture width is defined to be equal to the sum of the thickness of layers that the fracture is present in. Propagation through layer boundaries is accounted for by varying P_{trunc}. For a given values of P_{trunc}, it is the largest fractures that are permitted to propagate.

Table 1. Modelled fracture properties

Orientation	Strike uniformly distributed in the range NW-SE ± 15° and dip=86°
Length	Power-law: L_{max}=50-200m, L_{min}=1-50m, m =1.8-4.5 (single values selected for each realisation)
Density	1 – 5 m^{-1} Poisson distributed

The effect of the length distribution on percolation is investigated by assuming all fractures to be open and assuming a power-law distribution for fracture length. L_{max} is constrained by mud-loss data to between 50 and 200 m, L_{min} is unknown and m is assumed to vary between 1.8 and 4.5 with a maximum likelihood around 3.0 [15]. Therefore, a value is selected from the ranges shown in Table 1 to define a power-law length distribution for each realisation. An example of a single layer within a fracture network realisation including a magnified section is shown in Figure 3.

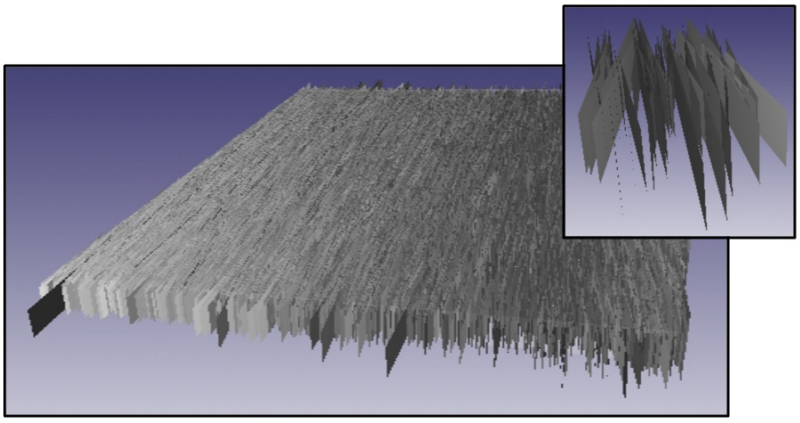

Figure 3. A single fracture network realisation with properties selected from the distributions shown in Table 1.

Results of fracture modelling show that increasing the mean length of fractures increases the fracture network connectivity. For fracture networks with densities of 1 m^{-1}, horizontal percolation over the model region is found to occur for length distributions with mean lengths of roughly 30m or more. Increasing the density to $5m^{-1}$ results in horizontal percolation for length distributions with mean lengths of roughly 5 m or more. Figure 4a displays a realisation with L_{mean} = 200 and Figure 4b displays a realisation with L_{mean} = 25. Currently, the only available length data is from mud losses which find maximum values of fracture length and so it is not possible to ascertain whether fracture lengths are great enough to cause percolation. However, it may be possible to confine fracture length by estimating the average fracture surface area from image data [17].

Vertical percolation is dependent on the value of P_{trunc}. Modelling finds that vertical percolation requires at least one fracture from a percolating cluster within a layer to also be present in the percolating cluster of an adjacent layer. Therefore, for any realisations which are already horizontally percolating, any non-zero value of P_{trunc} will provide vertical percolation. It may be possible to ascertain an estimate of P_{trunc} from image data.

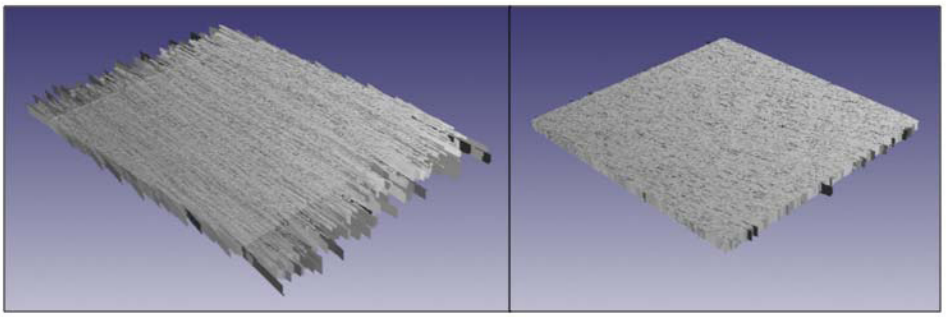

Figure 4. Fracture network realisation with (a) L_{mean} = 200 (b) L_{mean} = 25.

The results described so far assume fracture networks where all fractures are open. However, as discussed in Section 2, core data shows that some fractures are closed. Closed fractures act to (a) reduce the density of open fractures and (b) form barriers to flow. Additionally, it is reported that other more randomly oriented fractures are present in the region although they are not characterised. The random orientation implies that these fractures will be oriented with greater components perpendicular to the maximum principal stress and so are more likely to be closed. These factors mean that even if fracture lengths exceed those calculated previously, percolation may not occur. Additionally it should be noted that the uncertainty in the fracture properties is due to both epistemic uncertainty and variability over the region that fracture data was collected. However, it does not take account of variability across the wider area such as clustering or orientation variation. Therefore, the modelling performed here can only be considered truly representative around the wellbore region.

For the reasons discussed in this section, there is uncertainty over whether a percolating fracture network exists or not over significant distances within the reservoir and lower caprock. The uncertainties are largely contained in the length distribution,

the proportion of cemented fractures and properties of the other disperse fracture set. If a percolating pathway does exist and capillary entry pressures are exceeded for this pathway then flow will be expected to occur through the pathway. The permeability of the pathway, if well connected, will be largely dependent on the aperture distribution of the fractures and could be estimated with the Oda approximation [18]. If a percolating pathway does not exist over large distances then permeability in the region will be highly variable and a numerical permeability solution will be appropriate. Note that it is within the lower caprock that permeability is significantly dependent on percolation. Within the reservoir, the permeability may not be significantly affected by whether the network is percolating or not as all the open fractures can contribute to permeability [19].

5. Injection induced changes in the fracture network

As discussed in Section 2, injection of CO_2 into the reservoir will change the stress state with the potential for geomechanical failure of fractures and/or changes in fracture network properties. Stress change is particularly dependent on the permeability and elastic moduli of the region. To assess stress change thoroughly would require a dual porosity dual permeability model coupled with geomechanics and consideration of uncertain and time varying permeability. Instead, a computationally feasible approach is applied here that uses a single porosity single permeability model coupled with geomechanics assuming linear elastic behaviour. With this model, a small number of scenarios of the permeability and elastic moduli are run to estimate the uncertainty in the stress change. Fracture failure is then assessed following the methodology of Smith et al. [16] which combines modelled stress and pressure changes with uncertain data on mechanical properties and the pre-injection stress state.

Pre-injection reservoir pressure is 17.5 MPa [1]. Pre-injection stresses are subject to large uncertainties and are estimated from graphs provided in an internal report on geomechanics assessment of the site. Minimum horizontal stress (σ_3) is in the NE-SW direction and is estimated to be in the range 24 – 31 MPa. Maximum horizontal stress (σ_1) is in the NW-SE direction and is estimated to be in the range 44 – 48 MPa. These values are shown in Table 2. The angle of internal friction is estimated to be in the range 35 - 40º.

In assessing injection induced stress change, KB-502 is focussed on, although the general methodology is applicable to each injection well. It is assumed that any reservoir and lower caprock fracture networks are not connected together vertically so that CO_2 flow occurs in the reservoir only. This is modelled by setting high caprock capillary entry pressures. This is a conservative assumption with regards to pressure increase and failure. Four scenarios are modelled in total, formed by combing two permeability and two elastic moduli scenarios. Both permeability scenarios contain a thin corridor of $k = 1 - 4 \times 10^{-12}$ m^{-2} between KB-502 and KB-5 to account for the breakthrough observation [2]. The first permeability scenario assumes a reservoir permeability contribution from the matrix only, $k = 1\text{-}2 \times 10^{-14}$ m^{-2}. This is unlikely but sets an upper limit on stress changes. The other permeability scenario assumes that fractures contribute significantly to reservoir permeability, $k = 2\text{-}10 \times 10^{-13}$ m^{-2} in the NW-SE direction. As discussed in the previous section, this permeability scenario is more likely although the exact value of the fracture permeability contribution is uncertain. Reports on core analysis suggests E in the range 12 – 47 GPa and υ in the range 0.09 – 0.33. The elastic moduli scenarios have constant values of E and υ throughout the model. One with maximum values of E and υ and the other with minimum values of E and υ.

The coupled flow-geomechanical model used is formed of 50x50x20 grid blocks with local grid refinement such that the central grid blocks have horizontal area of 2,500m^2 and the total model width is approximately 600km. Rock and fluid properties represent the current state of knowledge. Zero displacement boundary conditions are applied to the horizontal sides and base of the model. Injection of CO_2 at the site is modelled over four years using ECLIPSE, an industry standard coupled flow-geomechanical numerical simulator.

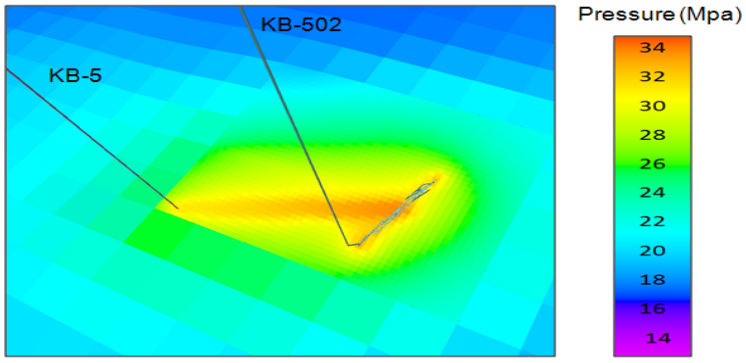

Figure 5. Reservoir pressure distribution in the low permeability injection scenario at time of maximum pressure.

Stress and pressure changes directly around the well are considered as these represent the region undergoing the greatest pressure change. The likelihood of failure decreases with distance from this region. The maximum modelled pressure change is 7.5 MPa for the high permeability scenario and 17 MPa for the low permeability scenario. Reservoir pressure distribution at the time of maximum pressure is shown in Figure 5. The modelled horizontal stress changes around KB-502, accounting for

uncertainty in E and ν, are in the range 3.9 – 6.4 MPa for the high permeability scenario and 8.9 – 14.3 MPa for the low permeability scenario. These values are shown in Table 2.

Table 2. Pre-injection pressure/ stresses and injection induced changes in stress/pressure. All units are MPa.

Initial state			High permeability		Low permeability	
σ_1	σ_3	P	$\Delta\sigma_1 / \Delta\sigma_3$	ΔP	$\Delta\sigma_1 / \Delta\sigma_3$	ΔP
44 - 48	24 - 31	17.5	3.9 - 6.4	7.5	8.9 – 14.3	17

Shear and tensile failure is assessed using the conditions described in Section 2. Results show that geomechanical failure of the in-tact rock is very unlikely to occur and so it is failure of fractures that is investigated further here. For the tensile failure calculation, the pore pressure in the model is approximated to be equal to the fracture pressure. Fracture tensile failure is found not to occur for the high permeability scenario although pressure almost reaches the lower limit of σ_3. For the low permeability scenario, tensile failure of fractures is found to have a small likelihood of occurring. This is dependent on the initial value of σ_3 and the elastic moduli which affects $\Delta\sigma_3$. Even if failure is not occurring, the normal effective stress on fractures is reduced to low values for both scenarios. As experimental fracture stiffness data suggests that fracture stiffness is lowest at low confining stresses [9,10], the increase in fracture aperture could be significant. As another consequence of the low normal effective stress on fractures, only reasonably small shear stresses are required to cause fracture shear failure. Therefore, particularly in the low permeability scenario, shear failure of fractures is found to be possible. Shear failure of fractures is most likely for a high stress differential and for fractures at the greatest deviation from the NW-SE direction.

It is important to note the uncertainties inherent in this modelling. The lack of dual porosity dual permeability coupled modelling prohibits assessment of stress changes within different fractures. Additionally, the permeability scenarios used do not account for the change in permeability which occurs during injection. However, the results of the modelling provide some insight into the processes occurring during injection. In summary, if fractures contribute significantly to the pre-injection permeability of the reservoir then it is found that stress changes are unlikely to cause geomechanical failure of fractures in the reservoir or lower caprock. There will be fracture permeability enhancement although the magnitude of this is dependent on the fracture stiffness. Fractures however, may not contribute significantly to the permeability of the region pre-injection, perhaps due to very small or closed apertures, or small lengths. If this is the case then stresses have the potential to cause geomechanical failure of fractures which would lead to fracture widening. Potentially, this could cause fracture networks that were not already horizontally percolating to become so. Furthermore, if P_{trunc} is non zero then vertical percolation within the reservoir and lower caprock could be realised. This in combination with elastic widening of fractures could lead to significant permeability enhancement. However, if P_{trunc} is zero then stress changes are unlikely to lead to new propagation through layer boundaries and so the fracture network would remain unconnected vertically. It should be clarified that new fracturing into the upper caprock is not expected to occur and so leakage out of the storage complex via fractures is very unlikely. The only potential for this occurrence would be the existence of a pre-injection capillary sealed percolating fracture network in the upper caprock that became open to flow during injection. Data on upper caprock fracture properties would be required to assess this.

6. Conclusions

Fracture networks at In Salah are characterised in the context of general characteristics of fracture networks derived from other fracture network field measurements. Fracture modelling is then performed to create possible realisations of fracture networks in the reservoir and lower caprock. It is found that for open fractures, horizontal percolation is likely for fracture length distributions with mean values greater than 5 - 30 m, dependent on fracture density. However, the inclusion of closed fractures reduces the likelihood of percolation. Further fracture characterisation is required to better assess the existence of a horizontally percolating network. If a horizontal percolating network exists and P_{trunc} is non zero then vertical percolation will occur through the reservoir and lower caprock. Coupled flow-geomechanical modelling of injection provides estimation of the range of stress changes expected in the region. Assessment of geomechanical failure finds that tensile failure of fractures is unlikely although the low effective stresses produced by injection will cause fracture aperture to increase. Additionally, this makes shear failure of fractures possible which could further increase their aperture. New induced fracturing into the upper caprock is not expected to occur and so leakage out of the storage complex via fractures is very unlikely. The only potential for this occurrence would be the existence of a pre-injection capillary sealed percolating fracture network in the upper caprock that became open to flow during injection but more data would be required to assess this.

Acknowledgements

Research reported in this paper was carried out within the framework of European Commission funded project CO2ReMoVe (SES6-2005-CT-518350). Further funding was provided by the EU Marie Curie Research Training Network GRASP (MRTN-CT-2006-035868). The authors wish to thank the EU, the In Salah Gas Joint Industry Project (BP, Statoil, Sonatrach) and CO2ReMoVe project partners for their support and contributions towards their research.

References

[1] Iding, M., Ringrose, P., 2010. Evaluating the impact of fractures on the long-term performance of the In Salah CO_2 storage site. Int. J. Greenhouse Gas Control. 4, 242-248.

[2] Ringrose, P., Atbi, M., Manson, D., Espinassous, M., Myhrer, O., Iding, M., Mathieson, A., Wright, I., 2009. Plume development around well KB-502 at the In Salah CO_2 storage site. First break. 27, 49-53.

[3] Mathieson, A., Midgley, J., Dodds, K., Wright, I., Ringrose, P., Saoul, N., 2010. CO_2 sequestration monitoring and verification technologies applied at Krechba, Algeria. The Leading Edge. 29(2), 216-222.

[4] Bonnet, E., 2001. Scaling of fracture systems in geological media. Rev. Geophys.. 39(3), 347.

[5] Barton, C. C., Zoback, M. D., 1990. Self similar distribution of macrosscopic fractures at depth in crystalline rock in the Cajon pass scientific drillhole. Rock Joints.

[6] Marret, R., Ortega, O., Kelsey, C., 1999. Extent of power-law scaling for natural fractures in rock. Geology. 27(9), 799-802.

[7] Baghbanan, A., Jing, L., 2007. Hydraulic properties of fractured rock masses with correlated fracture length and aperture. Int. J. Rock Mech. Min. Sci. 44(5), 704-719.

[8] Vermilye, J. M., Scholz, C. H., 1995. Relation between vein length and aperture. J. Struct. Geol. 17. 3, 423-434.

[9] Bandis, S. C., Lumsden, A. C. and Barton, N. R., 1983. Fundamentals of rock joint deformation. Int. J. Rock Mech. Min. Sci. & Geom. Abst. 20(6), 249-268.

[10] Baghbanan, A., Jing, L., 2008. Stress effects on permeability in a fractured rock mass with correlated fracture length and aperture. Int. J. Rock Mech. Min. Sci. 45(8), 1320-1334.

[11] Jaeger, J. C., Cook, N. G. W., Zimmerman, R. W., 2007. Fundamentals of Rock Mechanics, third ed. Blackwell Publishing.

[12] Robinson, P. C., 1984. Numerical calculations of critical densities for lines and planes. J. Phys. A: Math. Gen. 17, 2823–2830.

[13] Berkowitz, B., 1995. Analysis of fracture network connectivity using percolation theory. Math. Geol. 27(4), 467-483.

[14] Huseby, O., Thovert, J. F., Adler, P. M., 1997. Geometry and topology of fracture systems. J. Phys. A: Math. Gen. 30(5), 1415-1444.

[15] Mourzenko, V. V., Thovert, J. F., Adler, P. M., 1997. Percolation of three-dimensional fracture networks with power-law size distribution. J. Struct. Geol. Phys. Rev. E. 72. 036103

[16] Smith, J., Durucan, S., Korre, A., Shi, J-Q. 2010. Carbon dioxide storage risk assessment: Analysis of caprock fracture network connectivity. Int. J. Greenhouse Gas Control (under review).

[17] Ozkaya, S. I., Mattner, J., 2003. Fracture connectivity from fracture intersections in borehole image logs. Comput. Geosci. 29(2), 143-153.

[18] Oda, M., 1985. Permeability tensor for discontinuous rock masses. Géotechnique. 35, 483.

[19] Kamath, J., Lee, S. H., Jensen, C. L., Narr, W., Wu, H., 1998. Modeling fluid flow in complex naturally fractured reservoirs. SPE India Oil and Gas Conference and Exhibition, 17-19 February, New Delhi, India, SPE 39547-MS.